

DEVELOPMENT OF A MONOLITHIC, PROGRAMMABLE SAW FILTER IN SILICON

J.C. Haartsen

Delft University of Technology, Electrical Engineering Dept.
P.O. Box 5031, 2600 GA Delft, the Netherlands

ABSTRACT

In this paper the development of a monolithic, programmable Surface-Acoustic-Wave (SAW) filter in a ZnO-SiO₂-Si layered structure is presented. Two programmable taps with integrated detection-control capabilities are discussed, producing efficiencies of 40-50 dB with a control range of 15-20 dB at 100 MHz. They consist of implanted pn junction electrodes at the silicon surface and have a smooth surface for an unperturbed SAW propagation.

A new SAW generating transducer is proposed with a combined junction-metal interdigital pattern. A large dielectric medium under the transducer is created by the depletion regions of the reverse-biased junction pattern. In this way optimal efficiency of SAW transducer and taps can be obtained.

Experimental results are given for a 16-tap, full silicon programmable filter operating at 100 MHz.

I. INTRODUCTION

In modern communication receivers programmability of filter functions is highly desirable. It enhances the flexibility and allows adaptive signal processing. Real-time change of codes in matched filters improves the security in Spread-Spectrum and radar systems, whereas periodical adjustment of the filter function in adaptive filters reduces the deterioration of a-priori unknown or time-varying interference and multipath distortions.

Sophisticated filter functions for the above-mentioned systems can be realized with the transversal filter. The most direct and asynchronous implementation of such a filter is the Tapped Delay Line. In this filter the signal is periodically sampled at equidistant taps. After multiplication of each tap output with an arbitrary weight factor, the tap outputs are superposed in a common summation circuit. By choosing the tap weight factors appropriately a wide variety of filter functions can be obtained. If the tap weight factors can be changed electronically a *Programmable Tapped Delay Line* (PTDL) results. For filter bandwidths up to a few MHz, PTDLs can be realized with digital LSI circuitry or analog Charge-Transfer devices. However, at higher operating frequencies and wider bandwidths high power consumption results. In the frequency range 50-500 MHz Surface-Acoustic-Wave (SAW) technology provides an attractive alternative.

A SAW implementation of a PTDL is shown in Fig. 1. An Interdigital Transducer (IDT) converts the electric input signal into an acoustic wave, which is subsequently sampled by the taps in the propagation path. In the past, hybrid configurations with a separate SAW TDL on a piezoelectric substrate and external tap-control electronics were developed. Monolithic implementations are more attractive. Although their performance has not yet reached the status of the hybrid configurations, they will ul-

timately give the best results with respect to reliability, cost-effectiveness and filter performance.

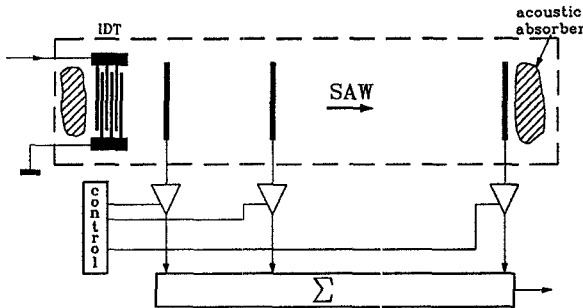


Fig. 1: Basic SAW PTDL configuration.

In this paper the development of a full silicon PTDL is described. Thin ZnO films are used to provide the piezoelectricity required for the acoustoelectric conversion processes. In this ZnO-SiO₂-Si layered structure a complete merging of acoustic and electronic signal processing is possible. Firstly, the programmable taps are considered. Secondly, the SAW generation at the input of the TDL is discussed. Finally, the complete monolithic filter is described.

II. ACTIVE SAW DETECTION

The key element of the PTDL is the programmable tap. In this component the acoustical signal is converted into an electrical signal, and the output amplitude is electronically controlled to add a certain weight factor. In hybrid configurations these functions are separated: a passive detector in the SAW propagation path and external control electronics. The passive detection takes place by capacitive coupling between the SAW potential and a conductive electrode. The electrical output signal is completely determined by the acoustical input power P_i^A and the conversion efficiency of the detector, see Fig. 2a. Low efficiencies are required to assure an unperturbed propagation of the SAW ($P_i^A = P_i^E$) and to avoid regeneration of acoustic waves, which is caused by the reciprocity of the acoustoelectric conversion mechanism in this passive detector.

In the active detector the acoustic wave modulates a much stronger electrical power flow, see Fig. 2b. The output signal is not only determined by the incoming acoustic power, but also by an auxiliary, electrical power source P_{aux}^E . As a consequence a high output signal results without the extraction of power from the wave. In addition, regeneration is avoided due to the irreversibility of the modulation process. Amplitude control can simply be achieved by controlling the auxiliary power supply P_{aux}^E . Thus in the active tap the detection and weighting functions can be inte-

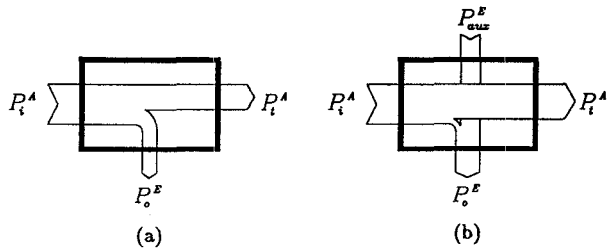


Fig. 2: Passive (a) and active (b) detection mechanisms. P_i^A and P_o^A are the in- and outgoing acoustic power flows.

grated into a single element. Due to the compact structure RF signal processing can be concentrated in a restricted area, which minimizes EM feedthrough and parasitic losses.

Because in the $\text{ZnO}-\text{SiO}_2-\text{Si}$ structure electronic components can directly be placed in the SAW propagation path new, active detection mechanisms can be applied in which the electric fields of the SAW directly interact with the mobile charge carriers of the semiconductor devices. Acoustic and electronic processing functions are fully merged in these *piezotronic* elements.

III. PROGRAMMABLE JUNCTION TAPS

Junction Electrodes

The taps in the propagation path produce a periodic disturbance of the wave impedance, which results in intertap reflections and distortion of the filter function. In conventional SAW devices the detectors consist of conductive, metal electrodes, which give rise to reflections at the electrode edges due to the step discontinuity and due to the change in elastic and electrical conditions (mechanical and electrical loading). Usually the electrical loading can be ignored due to the weak coupling in active taps.

In the $\text{ZnO}-\text{SiO}_2-\text{Si}$ structure metal electrodes can be avoided by using highly conductive, diffused or implanted electrodes located at the SiO_2-Si interface. In this way disturbances due to topological discontinuities and mechanical loading are minimized. A small mechanical loading remains due to the change in the shear elastic constants caused by the doping effect (1), see Fig. 3. This picture shows the calculated, mechanical reflection coefficient r_m at the edge of a diffused electrode with a donor or acceptor concentration of $1 \cdot 10^{20} \text{ cm}^{-3}$ in a substrate of $1 \cdot 10^{14} \text{ cm}^{-3}$ as a function of the junction depth d_j . In addition, the edge reflection coefficient of an aluminum electrode situated at

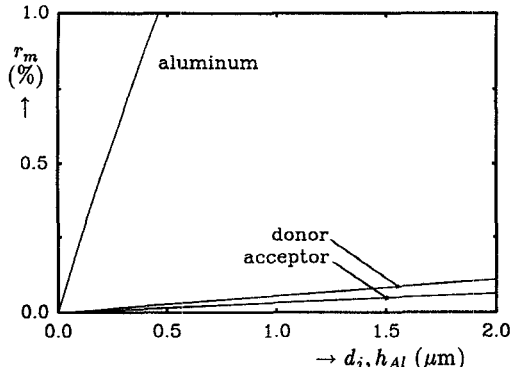


Fig. 3: Mechanical reflection coefficient for an aluminum and junction electrode with doping concentrations $N_a, N_d = 1 \cdot 10^{20} \text{ cm}^{-3}$ as a function of the aluminum thickness h_Ai and junction depth d_j , respectively.

the $\text{ZnO}-\text{SiO}_2$ interface is depicted. In both cases the ZnO thickness is taken $10 \mu\text{m}$, the SiO_2 thickness is ignored and a 100 MHz SAW in a (100)[001] Si substrate is assumed. The calculated data was obtained by determining the SAW velocity change due to the change in elastic constants in the layered structure.

From Fig. 3 it can be concluded that for the practical electrode height $h_{Al} = 0.3 \mu\text{m}$ and junction depth $d_j = 1 \mu\text{m}$ the mechanical reflection coefficients differ by one order of magnitude. For the aluminum electrode the topological reflection coefficient should be added, which is absent in the smooth junction electrode. The smooth surface above the detector is also important with respect to the growth of high ZnO films and bulk wave scattering.

Now two implementation of active taps, which only use junction electrodes in the propagation path of the SAW will be discussed. These devices are made in an n^- -type epilayer on a p -type substrate.

The Barrier-Modulated Tap

The Barrier-Modulated Tap (BMT) is basically a planar reach-through diode. It consists of two highly-doped, implanted p^+ electrodes separated by a small gap (5 to $6 \mu\text{m}$), see Fig. 4. The electrodes are contacted at the ends to avoid metal parts in the SAW propagation path. When the reverse voltage at the drain is increased its depletion region will expand and finally it will reach the source electrode. In this case the n -region between the electrodes is completely depleted. At a further increase of the applied voltage the source is forwardly biased and starts to inject a thermionic emission current, which is exponentially dependent on the potential gap between source and drain. The DC operation corresponds to that of the BARITT diode, used for microwave oscillators (2). Due to the planar structure of the p^+np^+ structure the potential barrier will be minimal at the SiO_2-Si surface and as a result the injection current will be concentrated at this surface.

The electric fields accompanying a travelling SAW penetrate into the depleted gap and modulate the potential barrier, which results in a modulation of the lateral injection current. The sensi-

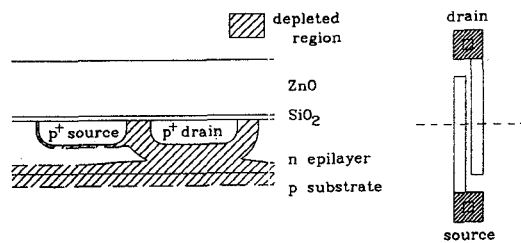


Fig. 4: Cross-section and top view of the Barrier-Modulated Tap.

tivity of the tap is proportional to the bias current which can thus control the output amplitude. Experiments in a $10 \Omega\text{cm}$ epilayer resulted in an untuned conversion efficiency of 45 dB with a 50Ω load at a 80 MHz operation frequency. Varying the bias current between 0 and 5 mA resulted in a 20 dB control range. An extensive discussion of this device can be found in (3).

The Junction FET Tap

In this device an implanted p^+ electrode forms the top gate of a Junction FET, see Fig. 5. Diffused n^+ electrodes form the source and drain electrodes. Apart from the top gate this FET has a bottom gate formed by the epi-substrate junction. For RF detection only the top gate is used, because of the high capacitance and low transconductance of the bottom gate. As a result a ring

configuration of the top gate is required, otherwise the channel can never be pinched off completely. A low output capacitance results if the drain is placed in the center of the ring. In contrast

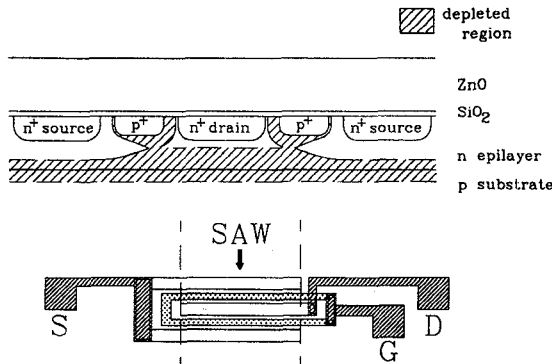


Fig. 5: Cross-section and top view of the Junction FET Tap.

to the BMT the JFETT has a buried channel in the bulk, which results in reproducible characteristics independent of the surface conditions.

The acoustic potential of the SAW capacitively couples to the top gate which then gives a modulation of the channel conductance. The top gate must be floating for AC operation. By controlling the DC bias voltage of the gate the sensitivity of the FET can be controlled. An optimal control range results if the bottom gate is fixed at the pinch-off voltage. Experiments at 95 MHz in a 10 Ω cm epilayer revealed an untuned conversion loss of 50 dB at a 50 Ω load. Varying the top gate voltage between 0 and 6 V resulted in a 15 dB control range. Detailed information can be found in (4).

The rather low sensitivity of the active taps can be attributed to parasitic loading due to test patterns, and due to the poor quality of the ZnO layers in the tap region as will be discussed in the next section. The control range of the taps was limited by the passive detection capability. When the bias conditions completely prevent active SAW detection, there remains the capacitive coupling of the SAW to the drains. The off value of the taps can be improved by using a dual-track configuration as will be discussed at the end of this text.

IV. SAW GENERATION

At the input of the PTDL the incoming electrical waveforms are converted into an acoustic surface wave. The most efficient transducer results when an InterDigital (ID) metal pattern is placed at the ZnO-SiO₂ interface. This configuration is also preferable when dispersion and fabrication complexity are taken into account, since the ZnO deposition can now be the final processing step. However, the silicon substrate forms a conductive medium which short-circuits the electric fields underneath the IDT. For optimal efficiency a thick, insulating SiO₂ layer is required.

The IDT efficiency can be investigated by determining the SAW velocity change $\Delta v/v$ when a perfectly conducting metal sheet is placed at the ZnO-SiO₂ interface. Figure 6 shows the $\Delta v/v$ as a function of the normalized oxide thickness wh_{ox} , when an optimal ZnO thickness of $wh_{ZnO} = 7500$ is assumed. The efficiency decreases with decreasing h_{ox} . However, the efficiency of the discussed junction taps increases with decreasing h_{ox} . This is

also shown in Fig. 6, where now the $\Delta v/v$ at the SiO₂-Si interface is determined and the silicon which now represents the depleted areas in the active taps is assumed insulating.

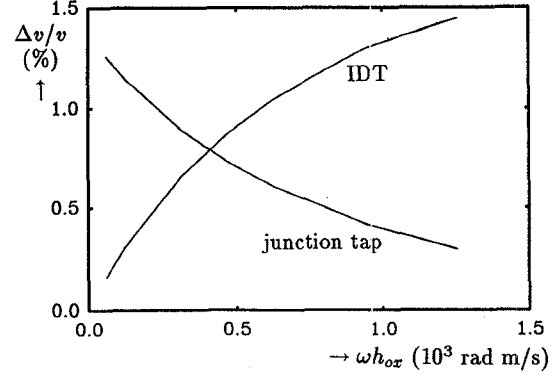


Fig. 6: The coupling strength $\Delta v/v$ for IDT at ZnO-SiO₂ interface, and junction tap at SiO₂-Si interface as a function of the normalized oxide thickness wh_{ox} .

In the monolithic filter discussed in the next section, both optimal coupling for the IDT and the junction taps is obtained by using a thick oxide layer of 2 μ m underneath the IDT and a thin oxide of 0.1 μ m in the remaining part of the filter where the taps are located. The introduced step in the propagation path: 1. gives rise to bulk wave generation; 2. requires a different periodicity of the IDT and the tap placement since the SAW velocity on the thin and on the thick oxide differs by more than 4%; 3. hinders the growth of uniform ZnO layers, since it depends on the substrate, and different growing conditions are required for the the 2 μ m and 0.1 μ m oxidized substrates.

To overcome these problems a new IDT configuration is proposed, which uses a thin oxide but still has its metal pattern at the ZnO-SiO₂ interface. In addition to a metal IDT pattern, a junction IDT pattern is placed, see Fig. 7. When the pn junction pattern is reverse biased a depletion region is created underneath the transducer. If an epilayer is present, an additional depletion

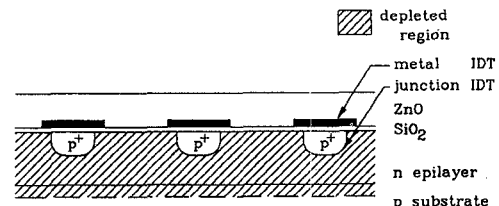


Fig. 7: Cross-section of the combined Junction-Metal IDT.

region around the epi-substrate junction can be built up from below. In this way the epilayer underneath this *Junction-Metal IDT* (JMIDT) becomes completely depleted and forms an excellent insulating medium for optimal SAW generation. In addition the thick dielectric layer is expected to reduce feedthrough, which mainly follows a path through the conductive substrate (5). The avoidance of a thick oxide is more compatible with standard IC processing, and due to the uniform oxide thickness in the propagation path a constant SAW velocity and uniform growth conditions for the ZnO layer are obtained.

V. MONOLITHIC PTDL

An experimental, monolithic PTDL was built and is shown in Fig. 8. Its dimensions are 10 x 10 mm. Conventional metal IDTs on a 2 μm thick oxide layer are applied. The active JFETTs and BMTs are implemented in a 10 Ωcm epilayer of about 10 μm thickness. A standard bipolar process was applied and only 6 pattern masks were required. The upper half of the chip consists of test patterns. In the upper part a delay line consisting of two SAW IDTs is discernable. In between JFETTs and BMTs are placed for testing purposes. At the bottom a PTDL consisting of one IDT and 16 BMTs has been placed. The drains of the BMTs are connected to a common output bar. The chip on the

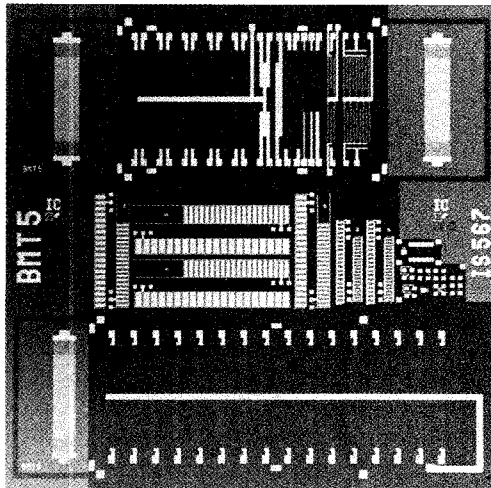


Fig. 8: Photograph of the monolithic implementation with test delay line in the upper part and 16-tap PTDL in the lower part of the chip.

photograph has not yet been covered with a ZnO layer.

The PTDL has an operating frequency of 115 MHz and a bandwidth of 10 MHz, which is determined by the IDT. The time domain measurement when the even numbered taps are alternately switched on and off is shown in Fig. 9. For this measurement the common drain was fixed at a constant DC voltage, while the sources were floating or switched to ground. When the taps were activated a bias current of 1 mA flew and a dissipation of 15 mW

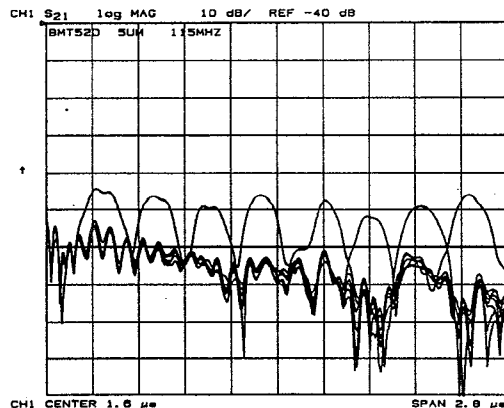


Fig. 9: Time domain measurement when the even-numbered taps are subsequently switched on and off.

resulted. The poor on-off ratio was caused by the passive detection mechanism. The off value can greatly be reduced by using a dual SAW track and two common bus bars of opposite polarity (6). The resulting common mode rejection will not only enhance the on-off ratio, but also reduce the feedthrough, which was quite large in this measurement. In this initial PTDL no counter measures against EM feedthrough were taken.

The ZnO sputtering conditions were optimized for the 2 μm oxide. This resulted in an irregular growth and grainy surface of ZnO above the 0.1 μm oxide regions. This explains the low efficiency in the BMTs as shown in Fig. 9. The ZnO thickness is about 5 μm . Due to the high feedthrough and passive detection processes no filtering results could be obtained with this preliminary experiment.

VI. CONCLUSIONS

In this paper the SAW generating and detecting part of a monolithic, programmable SAW filter have been highlighted. Active detection mechanisms in the taps avoid regeneration and provide a simple means of controlling the tap weight factor. Junction structures should be used to avoid discontinuities in the propagation path of the wave.

Conventional SAW transducers and the junction taps place opposing requirements on the SiO_2 layer thickness. A combined junction-metal transducer can be used to avoid these problems.

Measurements on a 16-tap monolithic SAW filter at 100 MHz demonstrated the feasibility of the implementation. In spite of the poor performance, the results are encouraging and improvements can be obtained by down-scaling the filter dimensions (higher frequencies, thinner ZnO layers), the application of a dual track to provide common mode and feedthrough suppression, and the improvement of the ZnO film growth.

ACKNOWLEDGEMENTS

The author wishes to thank the members of the Delft Institute for Microelectronics and Submicron Technology (DIMES) for their skillful processing and M.J. Vellekoop for depositing the ZnO layers.

REFERENCES

- (1) R.W. Keyes, "Electronic Effects in the Elastic Properties of Semiconductors," in *Solid State Physics*, vol. 20, F. Seitz, D. Turnbull, and H. Ehrenreich, Eds. New York: Academic Press, 1967, pp. 37-90.
- (2) J.L. Chu and S.M. Sze, "Microwave Oscillations in PNP Reach-Through BARITT Diodes," *Solid-State Electr.*, vol. 16, 1973, pp. 85-91.
- (3) J.C. Haartsen and A. Venema, "The Barrier-Modulated Tap: A New SAW Detection Method in Silicon," *Proc. IEEE 1988 Ultrasonics Symp.*, pp. 159-163.
- (4) J.C. Haartsen and A. Venema, "The Junction FET used as a SAW Detector in ZnO-SiO₂-Si Structures," to be published in the *Proc. IEEE 1989 Ultrasonics Symp.*
- (5) J.H. Visser and A. Venema, "Silicon SAW Devices and Electromagnetic Feedthrough," *Proc. IEEE 1988 Ultrasonics Symp.*, pp. 297-301.
- (6) D.E. Oates, D.L. Smythe, J.B. Green, "SAW/FET Programmable Transversal Filter with 100 MHz Bandwidth and Enhanced Programmability," *Proc. IEEE 1985 Ultrasonics Symp.*, pp. 124-129.